Design Optimization of Single-Phase Outer-Rotor Hybrid Excitation Flux Switching Motor For Electric Vehicles

Mohamed Mubin Aizat Mazlan, Erwan Sulaiman, Md Zarafi Ahmad,
Syed Muhammad Naufal Syed Othman
Universiti Tun Hussein Onn Malaysia, Locked Bag 101, Batu Pahat, Johor, 86400 Malaysia
mubinaizat@gmail.com, erwan@uthm.edu.my, zarafi@uthm.edu.my

***Abstract*—Nowadays, in-wheel motors applied in pure electric vehicles (EVs) propulsion systems have attracted great attention in advance research and development. In-wheel direct drive eliminates the mechanical transmission, differential gears and drive belts. Thus, in-wheel direct drive provides quick torque response, higher efficiency, weight reduction, and increased vehicle space. As one of alternative, a new design of hybrid excitation flux switching motor (ORHEFSM) for in-wheel drive EV is proposed. In this paper, the optimization design of single-phase 8S-4P outer rotor HEFSM is analysed. Open and close circuit of initial and final design is comparedbased on 2-D finite element analysis (FEA). The optimized design motor has produced higher torque which is 138.18Nm with 22.2% improvement compared to initial design motor which is 107.5Nm and has achieved the target value which 111Nm. The initial maximum power achieved was 17.02kW, while for the improved design motor, it has increased to 41.81kW, since the target maximum power is 41kW. The design optimization has been made on the initial design machine shows that there is great enhancement on torque and power.**

***IndexTerms*—Hybrid Excitation Flux Switching Motor, Electric Vehicle and Single-Phase Winding**

I. INTRODUCTION

By increasing number of population in the world, the demand toward vehicles for personal transportation has also been increased dramatically in the past of decade which leads to serious problems called 'global warming'. One of the main causes of global warming is Internal Combustion Engine (ICE). Through the report in year 2008 [1], about seven per cent of global carbon dioxide (CO_2) emission in year 2000 came from the vehicles. By the year 2015, it is expected that CO_2 emission rate from vehicles will increase two times with economic growth.

Hybrid Electric Vehicle (HEV) is considered as an ultimate eco- friendly car and this is highly expected to be popularized in the future [2]. The important of the basic characteristics requirements of an electric motor for HEV drive systems are high torque, high power density, and constant power at high speed as well as high efficiently [3].

Fig. 1 illustrated the main candidates of electric machine for HEV drive. Permanent Magnet Synchronous Machine (PMSMs) is used in HEV to overcome problem of low torque density and efficiency [4]. Although PMSM has the advantage of high torque density and high efficiency, still it has the problem of demagnetization and mechanical damage of rotor's magnet. Due to this reason, other alternative machine should be design to overcome the problems of PMSM already installed in HEV.

DC motors have been widely accepted in electric propulsion due to use battery as DC supply and simple control principle. However, DC motor drives have a few disadvantages such as low reliability, unstable current and high maintenance [5]-[6]. Thus DC motors are unsuitable for maintenance-free drives.

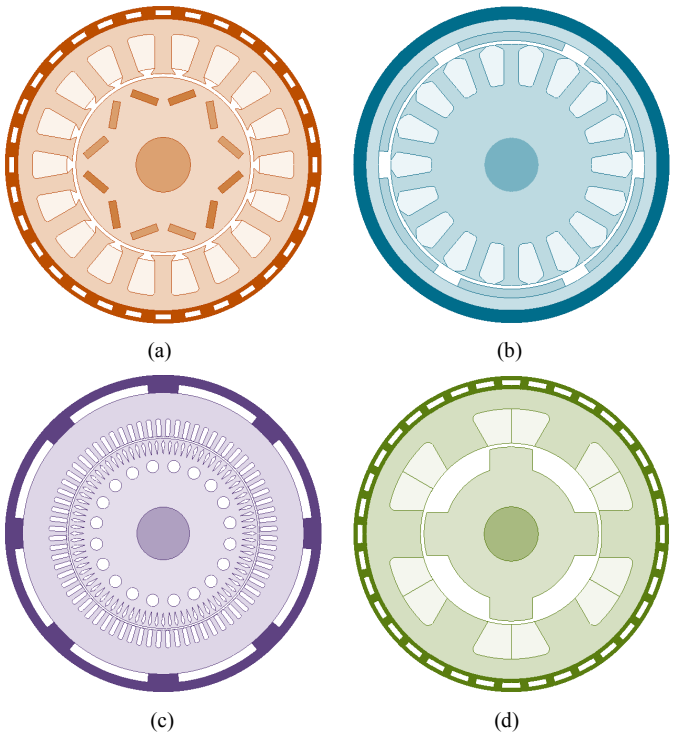

Fig. 1. Four Main Candidates of Electric Machine for HEV Drive
(a) Permanent Magnet Synchronous Machines (b) DC motor
(c) Induction Motor (d) Switched Reluctant Motor

978-1-4799-6428-4/14/$31.00 ©2014 IEEE

At present, induction motor (IM) are generally established as the most potential candidate for the electric propulsion of HEVs, due to their reliability, ruggedness, low maintenance, and low cost [7]. However, IM drives have demerits such as high loss, low efficiency and low power factor [8].

Then switched reluctant motor (SRM) is invented to overcome the permanent magnet problem. SRM has no PM and robust rotor structure but it is not suitable for HEV due to large torque ripples and noisy [9].

Electric vehicles (EVs) seem like an ideal solution to deal with the energy crisis and global warming since they have zero oil consumption and zero emissions. EVs have several advantages over Hybrid Electric Vehicles (HEV) such as EVs emit no tailpipe pollutants, although the power plant producing the electricity may emit them and EV provide quiet, smooth operation and stronger acceleration and require less maintenance than HEV. Therefore, Electric Vehicle (EV) is now regarded as an ultimate eco-friendly car and is widely expected to become more popular in the very near future [10].

However, most of commercial EV used single motor and transmission gears coupled to the wheels. This system leads to the transmission losses and reduce the efficiency and reliability of the motor. Therefore, in-wheel direct drive mechanism is introduced to overcome this problem. In-wheel direct drive eliminates the mechanical transmission, differential gears and drive belts.

Since the in-wheel direct drive with outer-rotor configuration is more practical for direct drive application, several invention of in-wheel mechanism for EV application has been proposed. For example 12S-22P outer-rotor permanent-magnet flux-switching machine (PMFSM) for electric propulsion in a lightweight electric vehicle has been proposed [11]. The proposed machine is a highly possible candidate for in-wheel direct-drivesThis PMFSM has physical compactness, robust rotor structure, higher torque and power density and high efficiency. However PMFSM has several disadvantages of uncontrolled flux and demagnetization [12].

Besides, 36S-24P outer-rotor permanent magnet (PM) hybrid machine also have been proposed [13]**.** This machine consist of permanent magnet (PM) and field excitation coil (FEC) as a main flux source has more advantage compared to PMFSM However this design have some disadvantage such as complicated design due to double-layer stator and high cost.

Thus, as one of the candidate that can overcome the problems, a new structure of outer-rotor hybrid excitation flux switching machine (ORHEFSM) with 8S-4P single-phase winding have been proposed [14]. The maximum torque achieved for initial design 8S-4P ORHEFSM is 96.8% of the target performance, whereas the maximum power is 17.02kW which is 41.51% of the target performance.In this paper, the optimization design of single-phase 8S-4P outer rotor HEFSM is analysed. Flux linkage of PM with DC FEC, flux line of PM only, induced voltage of PM with DC FEC, cogging torque, and torque and power versus FEC current density, J_E at various armature coil current densities, J_A for initial and final design is compared.

II. Operating Principle of ORHEFSM

The concepts of PMFSM and HEFSM have been introduced in the middle of 1950's [15] and in 2007 [16], respectively. The term "flux switching" is introduced due to the changing of the polarity of the flux linkage by following the motion of salient pole rotor.Outer-rotor HEFSM witha robust rotor structure similar with SRM is suitable for extreme driving condition [17]. The PM and FEC are placed at the stator and a simple cooling system can be used for this machines. In addition, FEC place the stator can control the variable flux abilities and have a potential to the torque and power. In the proposed ORHEFSM, the possible number of rotor pole and stator slot is defined by

$$N_r = N_s(1 \pm \frac{k}{2q}) \quad (1)$$

Where N_r is the rotor poles number, Ns is the number of stator slots, q is the number of phases and the natural number is defined as k. For the proposed motor, q is set as single phase, N_s is set as 8 and N_r is set as 4. In general, the rotation frequency of mechanical, f_m and the frequency of electrical, f_e for the proposed motor can be articulated as (2), where f_e, N_r and f_m is the frequency of electrical, number of rotor poles and mechanical rotation frequency, respectively.

$$f_e = N_r f_m \quad (2)$$

The operating principle of OR-HEFSM is demonstrated in Fig. 2. The red line indicates flux from PM and blue line indicates the flux from FEC, respectively. In Fig. 2(a) and (b), the polarity of both red and blue indicator are in the same direction.Thus, both of the PM and FEC fluxes are merged and flow together into the rotor. The combination of both fluxes generated more fluxes and called hybrid excitation flux. While in Fig 2(c) and (d), where the blue indicator is in reverse polarity and flow around the stator yoke, only the red indicatorof PM flux flows into the rotor which results in less flux excitation.

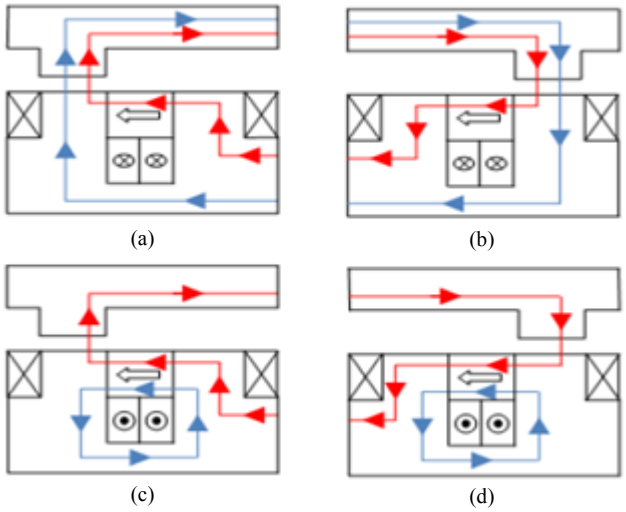

Fig. 2. Principle Operation of Outer-rotor HEFSM (a) θe = 0º (b) θe = 180º more excitation, (c) θe = 0º (d) θe = 180º less excitation

III. Design Restrictions, Specifications and Parameters of OR-HEFSM

Table I shows the electrical restrictions related with the inverter such as maximum 375V DC bus voltage and maximum 360A inverter current are set. The limits of the current densities areset to the maximum of $30A_{rms}/mm^2$ and $30A/mm^2$ for armature winding and DC FEC, respectively. In addition, the geometrical dimensions of the HEFSM such as the stator outer diameter, motor stack length, shaft radius and air gap are set to 264mm, 70mm, 30mm and 0.8mm respectively, while the PM weight is set to be 1.0kg. The target performance for maximum torque and power are 111Nm and 41kW respectively.

The commercial FEA package, JMAG-Designer ver.13.0, released by Japan Research Institute is used as 2D-FEA solver in this design. The material used for PM is NEOMAX 35AH with residual flux density and coercive force at 20 º are 1.2T and 932 kA/m respectively. Whereas for the stator and rotor body, the material used is electrical steel, 35H210.

Table II shows the parameters of the initial and final design of OR-HEFSM. From Table II, the rotor parameters involved are the outer rotor radius (D_1) which is 83% of the size of motor and within the range of general machine split ratio, rotor pole depth (D_2) which is more than the half size of the rotor and to ensure flux moves from stator to rotor equally without any flux leakage, the design of rotor pole arc width (D_3) is defined as in (3). The rotor pole width is reduced to allow optimal flux flows into the rotor pitch.

$$\sum Ws = \sum Wr \tag{3}$$

The distance between airgap and PM is (D_4). The PM slot shape parameters are the PM depth (D_5), and the PM width (D_6) calculated by using volume of 1kg PM. The size of both D_5 and $D_6$are reduced and expecting will give more flux to flow and increase the motor performances while for the FEC slot depth and FEC slot width, (D_7) and (D_8) calculated from (4). The area of optimized FEC slot is higher compared to initial design and give a maximum current density, J_e of 30 $A/mm^2$with 44 turns of FEC winding due to the flux have enough space to flow easily.

$$N_a = \frac{J_a \alpha S_a}{I_a} \tag{4}$$

Finally, the armature coil parameters are armature coil slot depth (D_9) and the armature coil slot width (D_{10}) calculated from (5) by using 168mm area of armature coil. The armature slot area is set similar for initial and final design in order to maintain the limitation of the maximum current densities which is set to $30A_{rms}/mm^2$. Therefore, the depth of D_9 is shorter is shorter and will prevent flux saturation while the shape of AC change to make the flux easily through it.

$$N_e = \frac{J_e \alpha S_e}{I_e} \tag{5}$$

TABLE I
HEFSM Design Restrictions

Items	Unit	8S-4P ORHEFSSM
Max. DC-bus voltage inverter	V	375
Max. inverter current	A_{rms}	360
Max. current density in armature winding, J_a	A_{rms}/mm^2	30
Max. current density in excitation winding, J_e	A/mm^2	30
Stator outer diameter	mm	264
Motor stack length	mm	70
Shaft radius	mm	30
Air gap length	mm	0.80
PM weight	kg	1
Maximum torque	Nm	>111
Maximum power	kW	>41

TABLE II
Outer Rotor Design Parameter of 8S-4P HEFSM

Parameter	Description	Initial	Final
D_1	Rotor outer radius (mm)	109.56	107.56
D_2	Rotor pole depth (mm)	10.82	16.15
D_3	Rotor pole width (mm)	64.22	55.45
D_4	Distance of airgap (mm)	0.80	0.80
D_5	PM depth (mm)	26.52	19.52
D_6	PM width (mm)	4.46	6.06
D_7	FEC slot depth (mm)	26.52	46.52
D_8	FEC slot width (mm)	5.53	7.30
D_9	AC slot depth (mm)	26.52	23.52
D_{10}	AC slot width (mm)	6.33	10.89
Area of FEC (mm^2)		147.67	339.60
Area of armature coil (mm^2)		168.93	144.16
FEC coil number (turns)		44	44
Armature coil number (turns)		7	6

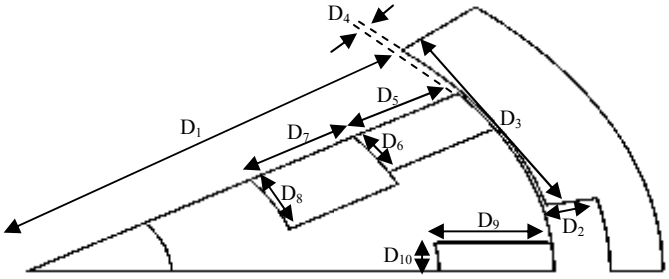

Fig. 3. Motor Design Parameter

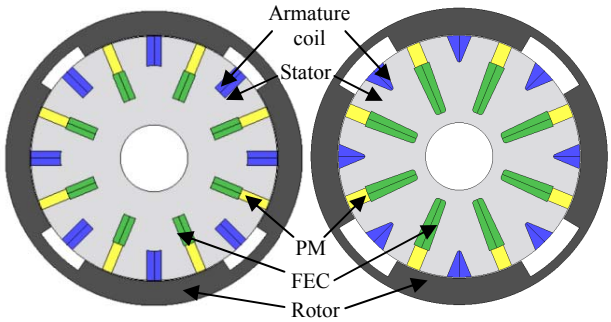

(a) (b)

Fig.4.8S-4P OR-HEFSM (a) Initial Design (b) Final Design

The motor design parameters, from D_1 to $D_{10}$are demonstrated in Fig. 3. Based on the motor parameters identified, the deterministic design optimization method is used and implemented using 2-D FEA solver to obtain the optimal performances of the proposed motor. In summary, the motor parameters D_1 to D_{10} are changed repeatedly until the target performances of torque and power are achieved. The initial and final design structure of ORHEFSM is illustrated in Fig. 4. Design Performance and Results Based on 2D Finite Element Analysis.

IV. Design Performance and Results Based on 2D Finite Element Analysis

A. Flux Linkage of PM and FEC

The flux linkage of the initial and final design at various condition of Je is plotted in Fig. 5. All the flux from PM has been successfully interacts with the FEC flux without any leakage. From these figure, it is showed that the magnitude of flux linkage of the final design at maximum Je has decreased 12.5% from 0.08Wb to 0.07Wb and the flux linkage of the final designed motor looks more sinusoidal compared with the initial design motor Hence, it has the ability to increase the performances of the motor.

B. Flux Path of PM

The field distribution for PM of initial and final design ORHEFSM is also analyzed and as shown in Fig. 6.From the both diagram, most of the flux flows at the stator around the FEC. The PM flux flows to the rotor of initial design higher compared to final design and generated higher induce voltage. Consequently, it reduces the amplitude of back-emf at open circuit condition even if the machine is operated under maximum speed condition.

C. Induced Voltage of PM with DC FEC

The comparison of back-emf of initial and final design ORHEFSM at the speed of 1200 r/min is investigated in Fig. 7. It is clearly shown that the amplitude of back-emf for the final design motor has significantly reduced from 43.74V to 36.36V. Furthermore, the back-emf of the final designed motor looks more sinusoidal compared with the initial design motor.The value of induced voltage must not exceed the supply voltage, 375V because it will interrupt the operation of the motors as it is use for regenerative breaking to charge battery.

D. Cogging Torque

The cogging torque of the final design ORHEFSM compared with the initial design is exemplified in Fig. 8. One cycle is formed as the rotor being rotate 360° electric cycle. The cogging torque generated is low which is good for the motor to produce low torque ripples. From the graph, the final design motor shows increment in peak-to-peak cogging torque ripple where it has increased 42% from 0.29Nm to 0.5Nm. Even the peak-to-peak cogging torque has increase, but the magnitude of peak-to-peak cogging torque is consider small if compared with the target ofmaximum torque.

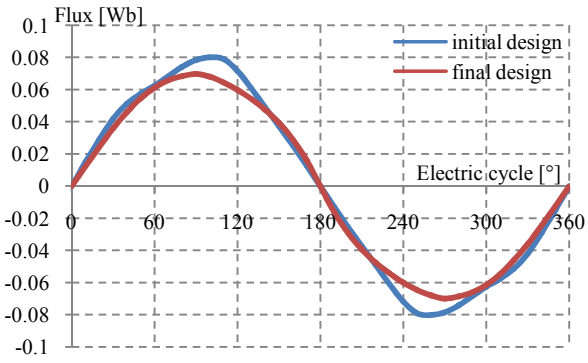

Fig. 5.Flux Linkage of PM with DC FEC with Various J_E

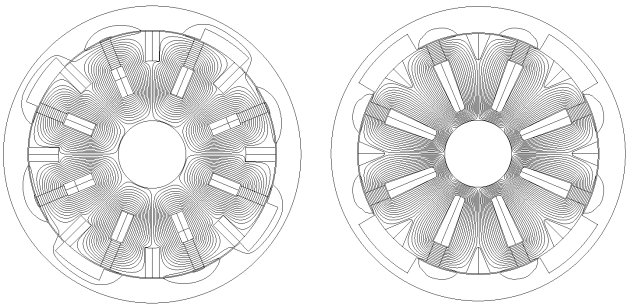

Fig. 6. Flux Path of PM in Open Circuit Condition (a) Initial Design (b) Final Design

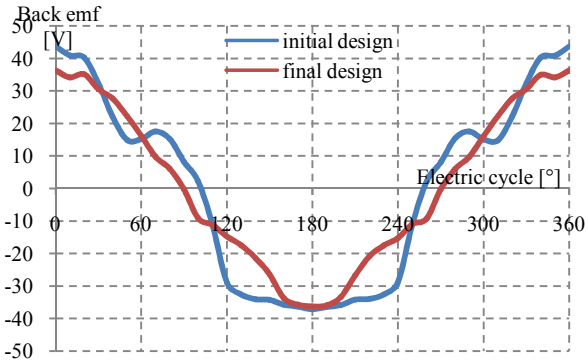

Fig. 7. Induced Voltage of PM with DC FEC

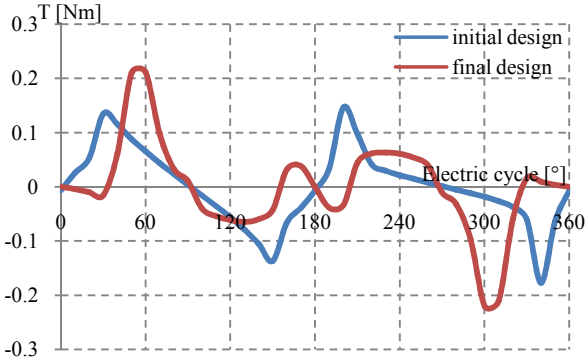

Fig. 8. Cogging Torque of PM Only

E. Torque and Power versus FEC Current Density, J_E at Various Armature Coil Current Densities, J_A

In load analysis, both FEC and armature coil current are supplied in the circuit with the values that have been calculated. From the torque value, the power value can be obtained. Both J_A and J_E are varied from 5A/mm^2 to 30A/mm^2 and 5Arms/mm^2 to 30Arms/mm^2, respectively. From Fig. 9, when J_A is set between 5 A_{rms}/mm^2 to 25 A_{rms}/mm^2, the output torque is reduced for Je greater than 15 A/mm^2. This phenomenon is due to the flux saturation effect.

The torque versus FEC current density at maximum $J_A$of the initial and final design is also compared and plotted as depicted in Fig. 10. The maximum torque obtained for the initial design is 107.5Nm, while the final design ORHEFSM is 138.18Nm and has achieved the target value which 111Nm. From the diagram, when J_A is set at maximum of 30 Arms/mm^2, the torque keep increasing as Je is increased from 0 A/mm^2 to 30 A/mm^{2}for both initial and final design.

Thus, the maximum power also has been increased and it has achieved the target value which 41kW as shown in Fig. 11. The initial design motor the maximum power achieved was 17.02kW, while for the final design motor, it has increased to 41.81kW and obtained when armature coil and DC FEC current densities are set to the maximum of 30Arms/mm^2 and 30A/mm^2. The torque and power is directly proportional to each other. From both graph, when $J_A$increase, the torque and the power increase smoothly.

Fig. 12 shows the torque and power versus speed. For the initial design ORHEFSSM, at base speed 1,512r/min, the torque obtained is 107.5Nm, while for the final design ORHEFSSM, at base speed 2,890r/min, the torque obtained is 138.18Nm as the maximum, respectively. Table III summarizes torque, power, weight, power density and torque density for target, initial and final design of ORHEFSM.

F. Motor Loss and Efficiency analyses

The motor loss and efficiency are computed by 2D-FEA considering copper losses in armature coil and FECs, and iron losses in all laminated cores. In Fig. 12, the specific operating points at the maximum torque, the maximum power, and frequent operating points under light load conditions are illustrated. For these operating points, the detailed loss analyses and motor efficiency of the finally designed machine are summarized in Fig. 13, where is the iron loss, is the copper loss, and is the total output power. At high torque operating points No.1, the motor efficiency is 96.24%. At high speed operating point No. 2, the motor efficiency is 87.73% with slight degradation due to increase in iron loss. Furthermore, at frequent operating points from No. 3 to No. 8, the proposed machine achieves relatively high efficiency approximately more than 92%. The proposed ORHEFSM can also work with high efficiency as much as 92% to 97%.

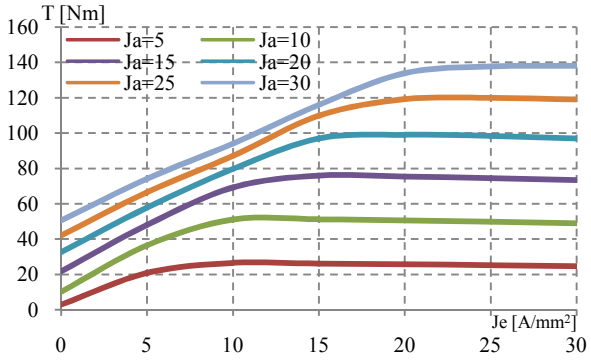

Fig. 9.Torque of PM with DC FEC at Various Armature Coil Current Densities, A/mm^2

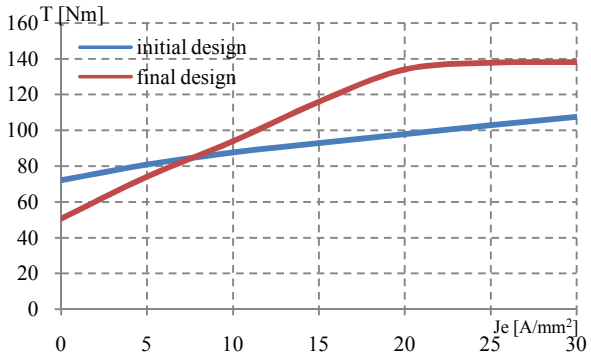

Fig. 10. Torque versus J_E at Maximum J_A

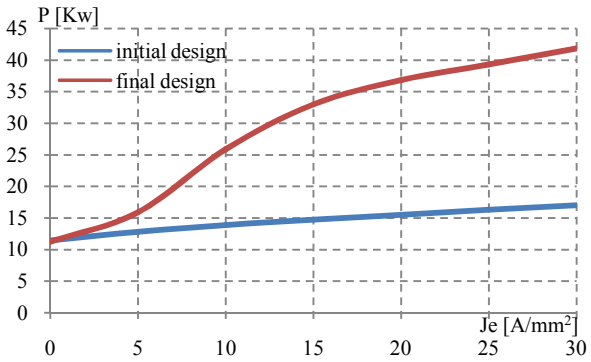

Fig. 11. Power versus J_E at Maximum J_A

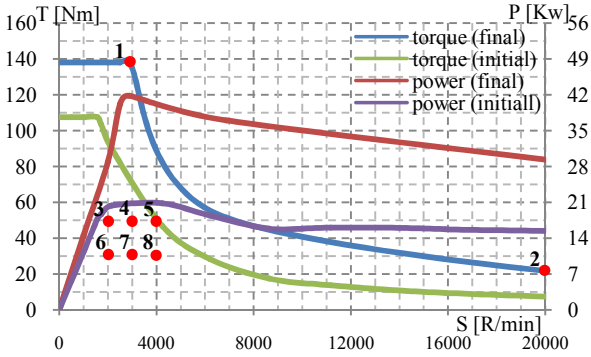

Fig. 12. Torque and Power versus Speed

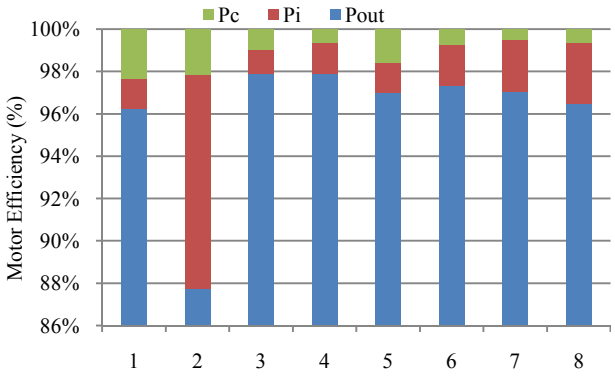

Fig. 13. Losses and Efficiency of The Final Designed Motor over Operating Points specified in Fig. 12

TABLE III
PERFORMANCE COMPARISON OF 8S-4P ORHEFSM

	Target	Initial	Final	% from target
T (Nm)	111	107.5	138.18	19.67%
P (Kw)	41	17.02	41.81	1.94%
Weight (kg)	35	27.87	28.41	18.83%
Pd (Kw/kg)	1.17	0.61	1.47	20.41%
Td (Nm/Kg)	3.17	3.86	4.86	34.77%

V. CONCLUSION

Design optimization studies of single-phase 8S-4P Outer-rotor HEFSM for in-wheel drive EV applications have been presented. The final design motor has produced higher torque which is 138.18Nm with 22.2% improvement compared to initial design motor which is 107.5Nm and has achieved the target value which 111Nm. The initial design motor the maximum power achieved was 17.02kW, while for the final design motor, it has increased to 41.81kW, since the target maximum power is 41kW.

ACKNOWLEDGMENT

This research was supported by GIPS (1369) under Research, Innovation, Commercialization and Consultancy Management (ORICC) UTHM, Batu Pahat and Ministry of Higher Education Malaysia (MOHE)

REFERENCES

[1] M. Z. Ahmad, E. Sulaiman, Z. A. Haron, and T. Kosaka, "Impact of rotor pole number on the characteristics of outer-rotor hybrid excitation flux switching motor for in-wheel drive EV", Proc of Int. Conf on Electrical Eng. &Infor., UKM, pp. 593-601, June 2013.

[2] M. Z. Ahmad, E. Sulaiman, Z. A. Haron, and T. Kosaka, "Design improvement of a new outer-rotor hybrid excitation flux switching motor for in-wheel drive EV", IEEE Int. Power Engineering and Optimization Conference, Langkawi, pp. 298-303, June 2013.

[3] M. Z. Ahmad, E. Sulaiman, Z. A. Haron and T. Kosaka, "Preliminary Studies on Permanent Magnet Flux Switching Machine with Hybrid Excitation Flux for Direct Drive Electric Vehicle Application", IEEE Int. Conf. on Power and Energy (PECON-2012), Sabah, pp. 928-933, Dec 2012

[4] W. Fei, P. Luk, and K. Jinupun, "A New Axial flux magnet segmented-armature-torus machine for in-wheel direct drive applications," IEEE Power Electronics Specialist Conference, pp. 2197-2202, 2008.

[5] C. C. Chan, "The state of the art of electric, hybrid, and fuel cell vehicles", *Proc. IEEE*, vol. 95, no. 4, pp.704–718, Apr. 2007.

[6] A. Emadi, J. L. Young, K. Rajashekara, "Power electronics and motor drives in electric, hybrid electric, and plug-in hybrid electric vehicles", *IEEE Trans. Ind. Electron.*, vol.55, no.6, pp.2237-2245, Jan. 2008.

[7] Jerry Bednarczyk, PE, Induction Motor Theory. Access on November 9, 2012. http://www.pdhonline.org/courses/e176/e176content.pdf

[8] C. C. Chan, "The state of the art of electric and hybrid vehicles", *Proc. IEEE*, vol. 90, no. 2, pp. 247–275, Feb. 2002.

[9] M. Z. Ahmad, E. Sulaiman, Z. A. Haron and T. Kosaka, "A New Structure of Outer-Rotor PMFSM with Hybrid Excitation Flux for In-Wheel Drive EV Applications", Proc. The 5th Int. Conference on Postgraduate Education (ICPE-5 2012), UTM, pp. 531-538, Dec 2012

[10] IEA-HEV Outlook, International Energy Agency Implementing Agreement on Hybrid and Electric Vehicles, "Outlook for hybrid and electric vehicles," 2008 [Online] Available: http://www.ieahev.org/pdfs/iahev_ outlook_2008.pdf

[11] W. Fei, P. Chi, K. Luk and J. S. Y. Wang, "A Novel Outer-Rotor Permanent-Magnet Flux-Switching Machine for Urban Electric Vehicle Propulsion," in *3rd International Conference on Power Electronics Systems and Applications (PESA)*, pp. 1–6, 2009.

[12] E. Sulaiman, T. Kosaka, and N. Matsui, "Design Optimization and Performance of a Novel 6- Slot 5-Pole PMFSM with Hybrid Excitation for Hybrid Electric Vehicle", *IEEJ Transaction on Industry Application*, Vol. 132 / No. 2 / Sec. D pp. 211-218, Jan 2012. (Scopus)

[13] Chunhua Liu, K. T. Chau, J. Z. Jiang, and LinniJian, ''Design of a New Outer-Rotor Permanent Magnet Hybrid Machine for Wind Power Generation'', *IEEE Transactions on Magnetics*, Vol. 44, No. 6, June 2008

[14] M. M. A. Mazlan, E. Sulaiman and T. Kosaka, ''Design Studies of Single-Phase Outer-Rotor Hybrid Excitation Flux Switching Machine for Hybrid Electric Vehicle'', IEEE Int. Power Engineering and Optimization Conference, Langkawi, pp. 138-143, March 2014

[15] S. E. Rauch and L. J. Johnson, "Design principles of flux switch altenators," AIEE Trans., vol 74III, no. 12, pp. 1261-1269, 1955.

[16] E. Hoang, M. Lecrivain, and M. Gabsi, "A New Structure of a Switching Flux Synchronous Polyphased Machine," in *European Conference on Power Electronics and Applications*, no. 33, pp. 1–8, 2007.

[17] E. Sulaiman, T. Kosaka, and N. Matsui, "Design Optimization and Performance of a Novel 6- Slot 5-Pole PMFSM with Hybrid Excitation for Hybrid Electric Vehicle", *IEEJ Transaction on Industry Application*, Vol. 132 / No. 2 / Sec. D pp. 211-218, Jan 2012. (Scopus)